

# Gas and Water Transport Properties of Epoxy–Amine Networks: Influence of Crosslink Density

CATHERINE DAMIAN, MARIELLE ESCOUBES, ELIANE ESPUCHE

Laboratoire des Matériaux Polymères et des Biomatériaux, UMR CNRS No 5627, Université Claude Bernard Lyon 1, 43 Boulevard du 11 Novembre 1918, F-69622 Villeurbanne Cedex, France

Received 20 June 2000; accepted 29 August 2000

**ABSTRACT:** The gas and water transport properties were studied on seven epoxy–amine networks that differ by their di/mono epoxy composition and their cure cycle. The characteristic parameters of transport  $M_{\infty}$  and  $D$  were determined in each case, and they show that the solubility and diffusion coefficients are influenced by their composition. The solubility increases with the extend of cure and with the decrease of dangling chains, and in both cases the evolution of the diffusivity is inverse. The variations of the solubility and diffusivity have been discussed as a function of two parameters: polar groups and unrelaxed holes of the glassy networks. © 2001 John Wiley & Sons, Inc. *J Appl Polym Sci* 80: 2058–2066, 2001

**Key words:** epoxy-amine networks; water and gas transport; sorption, permeation

## INTRODUCTION

The transport properties of water and small gases like O<sub>2</sub>, N<sub>2</sub>, and CO<sub>2</sub> have been studied on epoxy–amine networks in relation with the polymer structure. The water diffusion has already been studied in the literature<sup>1–6</sup> principally considering the specific interactions between the water molecules and the polar groups of the networks (hydroxyl, ether, amine). The chemical structure is then a fundamental parameter, and in that way, the polar groups concentration and the composition of the reactive system are the main parameters.<sup>2</sup>

The gas diffusion appears as a more original way to characterize the polymer matrix. In that case, the interaction approach is not the only one to be considered, because the gas transport in glassy polymers must take into account the presence of unrelaxed holes or free volumes, which

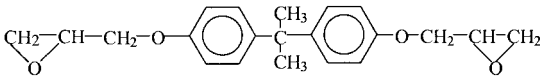
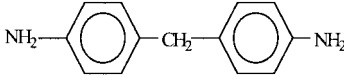
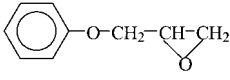
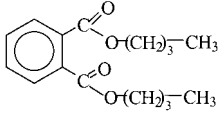
involve a volumetric approach. The free volumes theory has been initially developed on rubbery polymers using models based on the activation energy.<sup>2</sup> This last one is necessary either to create chains motions that provide a variation of free volumes allowing the gas diffusion or to create free holes whose sizes are higher than a critical value. In the glassy state, the chain motions are lower than in the rubbery one, and a higher energy seems necessary to create these motions. As the activation energy is of the same magnitude in both states, it can then be concluded that the gas molecules diffuse through unrelaxed holes with a low energy, and the dual mode has been developed to explain the sorption in glassy polymers.<sup>7,8</sup> According to this model, the gas molecules are sorbed in two ways: some gas molecules are fixed in the unrelaxed holes of the polymers that represent Langmuir sites, and the other gas molecules are sorbed according to Henry's law.<sup>9–11</sup> The transport depends then on the accessibility of these holes whose sizes correspond to those of gases. The physical characteristics of the polymer such as crosslink density, cohesive energy den-

---

Correspondence to: E. Escoubes.

*Journal of Applied Polymer Science*, Vol. 80, 2058–2066 (2001)  
© 2001 John Wiley & Sons, Inc.

**Table I Chemical Structure and Molecular Weight of the Different Components of Epoxy-Amine Networks**

Name of the Components	Chemical Structure	Molecular Weight (g/mol)
DGEBA (Bisphenol A diglycidyl ether)		348
DDM (4,4'-Diamino diphenyl methane)		198
PGE (Phenyl glycidyl ether)		150
DBP (Dibutyl phthalate)		278

sity, or rigidity of the chains must be taken into account,<sup>3</sup> and the gas diffusion studies can bring interesting relations with the network architecture.

## EXPERIMENTAL

The present study concerns, on one hand, a series of model epoxy-amine networks, differing by their crosslink density, and on the other hand, a

commercial network used for the embedding of low radiative wastes.

## Materials

The components used to prepare the networks are presented in the Table I.

All the networks are based on DGEBA as the epoxy prepolymer and on DDM as the comonomer. The monofunctional epoxy PGE with the same chemical structure as DGEBA has been in-

**Table II Molar Composition (Ratioed to 1 mol of Diamine DDM) and Weight Composition of Epoxy-Amine Networks: The Cure Cycles of the Epoxy-Amine Networks are Also Presented**

		DDM	DGEBA	PGE	DBP	Cure Cycle
A	mol	1	1.4	1.2	0.7	60 h at 60°C
	weight	19	47	17	17	
A <sub>r</sub>	mol	1	1.4	1.2	0	60 h at 60°C
	weight	23	56	21	0	+140°C on vacuum
B*	mol	1	1.4	1.2	0	60 h at 60°C
	weight	23	56	21	0	
B	mol	1	1.4	1.2	0	3 h at 80°C
	weight	23	56	21	0	+3 h at 130°C
B <sub>1</sub>	mol	1	1.1	1.9	0	3 h at 80°C
	weight	23	45	32	0	+3 h at 130°C
C*	mol	1	2	0	0	3 h at 80°C
	weight	22	78	0	0	+3 h at 130°C
C	mol	1	2	0	0	3 h at 110°C
	weight	22	78	0	0	+3 h at 190°C

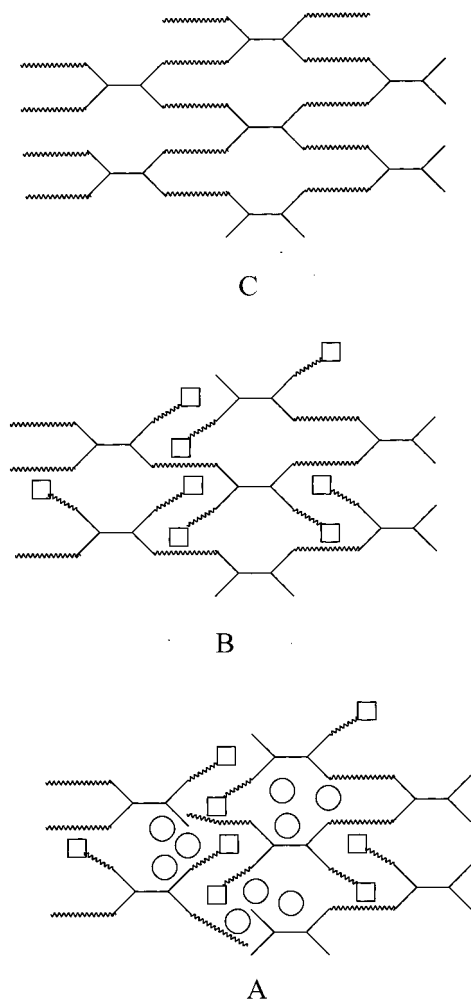


**Figure 1** Schematic representations of the architecture of the three main networks *A*, *B*, *C*.

produced in some systems to introduce unreactive dangling chains. The commercial network also includes an unreactive diluent DBP. Table II gives the composition of the seven different systems expressed in weight percent and also in number of mol ratioed to one mol of diamine. The epoxy group to amine group ratio is always equal to 2, which allows reaching the highest crosslink density for optimized cure cycles.

In all cases, the components are dissolved in acetone, and the films are obtained by casting the solution on glass plates. They are cured according to different cycles presented in Table II. The film thickness is equal to 20  $\mu\text{m}$ .

The studied networks are divided in three groups: (1) the networks *C* and *C\** are based on a difunctional epoxy DGEBA prepolymer, and they are differing by their cure cycles (*C* corresponds to the totally crosslinked network, and *C\** to the

untotally crosslinked one). The DSC analysis, performed at 10°C/min from  $-50^\circ$  to 200°C, gives glass transition temperatures equal to  $164 \pm 1^\circ\text{C}$  for *C* and  $145 \pm 1^\circ\text{C}$  for *C\**. For *C\**, an exothermic peak is observed, which indicates that the reaction is not complete at this first step. (2) The networks *B*, *B\**, and *B<sub>1</sub>* are based on DGEBA/

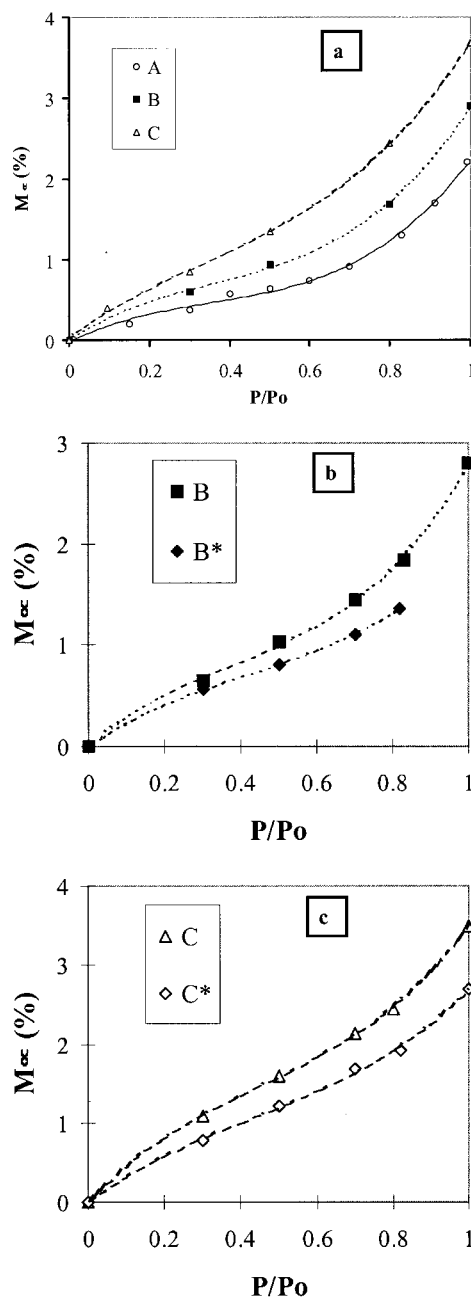


**Figure 2** Water sorption isotherms of the epoxy-amine systems *A*, *B*, and *C*. (a) Effect of the cure cycles on the sorption isotherms for the networks *B* (b) and *C* (c).

**Table III Water Sorption: Values of Equilibrium Content  $M_\infty$ , Diffusion Coefficient  $D$ , and Interaction Molar Energy  $\Delta H$  Obtained at Relative Pressures 0.3 and 0.8**

	$P/P_o = 0.3$			$P/P_o = 0.8$		
	$M_\infty$ (%)	$D$ ( $\times 10^9$ cm <sup>2</sup> /s)	$\Delta H$ (kJ/mol)	$M_\infty$ (%)	$D$ ( $\times 10^9$ cm <sup>2</sup> /s)	$\Delta H$ (kJ/mol)
A	0.40	—	67	1.17	4.43	63
B*	0.56	3.00	63	1.36	2.70	54
B	0.65	1.60	54	1.84	1.88	46
B <sub>1</sub>	0.63	1.58	—	1.51	1.66	—
C*	0.77	1.55	59	1.91	1.84	50
C	1.08	1.30	50	2.44	1.52	46

PGE/DDM (the monofunctional PGE content represents successively 46% by mol of the total epoxy component in *B* and *B\** and 67% in *B*<sub>1</sub>). The glass transition temperatures decrease with the content of PGE. They are equal to 120°C for *B*, 110°C for *B*<sub>1</sub>, and 87°C for the unfully cured network *B\**. (3) The systems *A* and *A*<sub>r</sub> correspond to commercial systems. The system *A* contains 17.6% by weight of DBP to decrease the viscosity and to allow the embedding of radiative wastes at temperatures lower or equal to 60°C. The glass transition temperature of the network *A* is equal to 60°C for a cure cycle of 60 h at 60°C. The determination of this temperature is difficult, due to the presence of different phenomena: endothermic phenomena such as water desorption, DBP departure, and exothermic effects due to the residual crosslinking reaction. The network *A*<sub>r</sub> corresponds to the network *A* from which DBP has

been taken off by heating at 140°C under vacuum. The glass transition temperature measured for *A*<sub>r</sub> is equal to that measured for the network *B* (117°C). Moreover, this network presents the same behavior as *B*, especially in sorption and permeation studies. So, we will only present and discuss the results obtained for *B*.

Figure 1 represents schematically the three main networks *A*, *B*, *C*, underlining the great proportion of dangling chains in the case of *B* and *A*. This proportion is even higher for the uncured networks.

## Methods

### Sorption Method

The samples are introduced in a SETARAM B92 microbalance, and the studies are made at a constant temperature (20°C) for water partial pressures ranging from 0 to 1, and for gas pressures ranging from 0 to 760 Torr.

The equilibrium weight uptakes give the sorption isotherm and a mean solubility coefficient (*S*) can be deduced from the mean slope of the isotherm.

During each equilibrium, the weight uptake, *M*(*t*), as a function of time gives the kinetical curves. The diffusion coefficient, *D*, can be deduced from the Fick's second law:

$$\frac{\partial C}{\partial t} = D \cdot \left( \frac{\partial^2 C}{\partial x^2} \right) \quad (1)$$

A simplified solution of this equation is obtained by introducing the following boundary conditions:<sup>12</sup> (1) the upstream surface equilibrium is reached instantaneously; (2) the concentration of sorbed molecules is equal to 0 for *t* = 0 at each

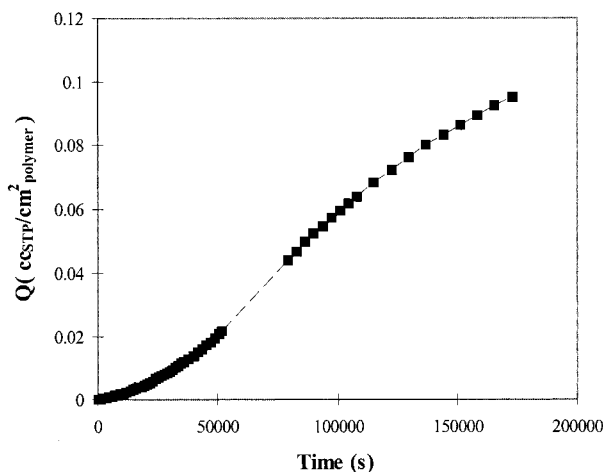


**Figure 3** Water transferred amount *Q* as a function of time for the network *B* in saturated water pressure condition.

**Table IV Water Transport Through the B Network: Permeability  $Pe$  and Diffusion Coefficient  $D$  Obtained under Saturated Pressure and Pervaporation Conditions**

	$Pe_{\text{slope}}$ (barrer)	$D_{\text{time-lag}}$ ( $\times 10^9 \text{ cm}^2/\text{s}$ )	$D_{\text{slope}}$ ( $\times 10^9 \text{ cm}^2/\text{s}$ )
Saturated pressure of water	30	0.20	0.19
Liquid water	25	0.20	0.19

The diffusion coefficients  $D$  are calculated from the time-lag method and from the slope of the curve  $Q = f(t)$ .

point inside the specimen; (3) the downstream surface desorption is instantaneous.

With  $e$ , the thickness of the film, one obtains:

$$\frac{M(t)}{M_\infty} = \left( 1 - \frac{8}{\pi^2} \times \sum_{n=0}^{\infty} \left[ \frac{1}{(2n+1)^2} \cdot \exp\left( \frac{-D \cdot \pi^2 \cdot (2n+1)^2 \cdot t}{e^2} \right) \right] \right) \quad (2)$$

The diffusion coefficient  $D$  and the equilibrium values  $M_\infty$  can be computed by iterative calculations leading to the best fit of the experimental data by the theoretical equation.

Complementary data can be obtained because the microbalance is coupled with a microcalorimeter thermostated at the same temperature. It is thus possible to measure the heat flow associated to the weight uptake during a pressure increment. The ratio of the heat flow to the weight uptake expressed in kJ/mol gives an experimental value of the differential sorption enthalpy  $\Delta H$ .

### Permeation Method

The permeation cell thermostated at 20°C consists in two compartments, separated by the studied membrane. A preliminary high vacuum desorption is carried out to ensure that the static vacuum pressure changes in the downstream compartment are smaller than the pressure changes due to the gas or water vapor diffusion.

Gas studies are performed under a  $6 \cdot 10^5$  Pa with a membrane area  $A$  of 3 cm<sup>2</sup>, and water studies are performed under saturated pressure or liquid (pervaporation conditions) with a membrane area  $A$  of 20 cm<sup>2</sup>.

In all cases, the pressure values in the downstream compartment allows obtaining the gas or vapor amount  $Q(t)$  that is diffusing through the

membrane as a function of time. This amount can be calculated by the integration of the second Fick's law under permeation conditions and a simplified form is obtained for very long times [eq. (4)].<sup>13,14</sup>

$$Q(t) = \left[ \frac{D \cdot t}{e^2} - \frac{1}{6} - \frac{2}{\pi^2} \times \sum_{n=1}^{\infty} \left( \frac{(-1)^n}{n^2} \cdot \exp\left( \frac{-D \cdot n^2 \cdot \pi^2 \cdot t}{e^2} \right) \right) \right] \cdot C_1 \cdot e \cdot A \quad (3)$$

$$Q = \frac{A \cdot D \cdot C_1}{e} \cdot \left( t - \frac{e^2}{6 \cdot D} \right) \quad (4)$$

where  $C_1$  is the sorbed concentration on the upstream face.

The characteristic curve  $Q = f(t)$  presents a transitory part followed by a linear one:<sup>13</sup> the permeability coefficient  $Pe$  is given by the slope of the straight line in the steady state, and the dif-

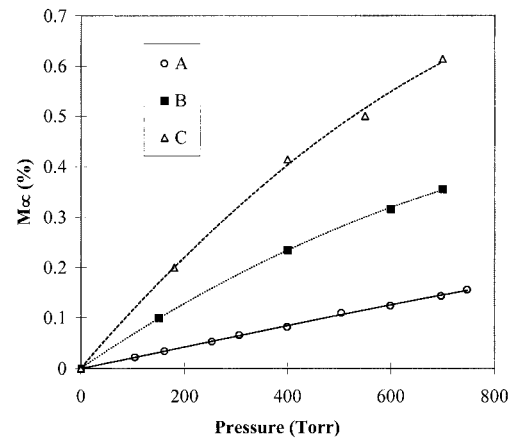


**Figure 4** The CO<sub>2</sub> sorption isotherms of the three epoxy-amine networks A, B, and C.

**Table V** CO<sub>2</sub> Sorption for the Networks *A, B, C*: Values of Equilibrium Content  $M_\infty$  and Diffusion Coefficient  $D$  for Pressures 400 and 700 T

	$P = 400 \text{ T}$		$P = 700 \text{ T}$	
	$M_\infty$ (%)	$D$ ( $\times 10^9 \text{ cm}^2/\text{s}$ )	$M_\infty$ (%)	$D$ ( $\times 10^9 \text{ cm}^2/\text{s}$ )
<i>A</i>	0.08	0.69	0.14	0.74
<i>B</i>	0.25	0.30	0.36	0.34
<i>C</i>	0.43	0.28	0.61	0.30

fusion coefficient  $D$  is obtained by the extrapolation of this straight line on the time axis, which is called the time lag “ $\theta$ .”

$$D = \frac{e^2}{6\theta} \quad (5)$$

In the absence of any permeate, the pressure increase in the downstream compartment is equal to  $5 \cdot 10^{-5}$  Torr/min. It corresponds to a fictive permeability that can be calculated according to the experimental conditions:  $2 \cdot 10^{-3}$  barrers for CO<sub>2</sub> and 10 barrers for water. These values give the limit values that can be measured in each case.

The present analysis is developed according to the dissolution–diffusion theory in dense films. Nevertheless, some authors<sup>15</sup> have applied to epoxy–amine networks the diffusion theory developed for porous media. In this case, the effective part of a volume  $dV$  participating to the transport is  $\varepsilon dV$ ,  $\varepsilon$  being the microporosity, and the second simplified Fick’s law can be expressed:

$$Q = \frac{A \cdot D \cdot C_1}{e} \cdot \left( t - \frac{\varepsilon \cdot e^2}{6 \cdot D} \right) \quad (6)$$

$C_1$  is in that case the liquid or vapor concentration in the upstream phase.

The  $C_1$  values are very different in pervaporation and permeation conditions, and they are both

distinct from the sorbed concentration value in the upstream surface layer.

The diffusion coefficients determined from the “time lag”  $D_{\text{time-lag}}$  correspond to  $D/\varepsilon$ . In both conditions, they must be much higher than the  $D$  values obtained from the slope of  $Q = f(t)$ :

$$D_{\text{slope}} = \frac{\partial Q}{\partial t} \cdot \frac{e}{A \cdot C_1} \quad (7)$$

## WATER TRANSPORT RESULTS

### Sorption Analysis

Figure 2(a) represents the water isotherms of *A, B, C*, and Figure 2(b)–(c) show the effects of the cure cycle for *B* and for *C*. Table III gives, for the partial pressures 0.3 and 0.8, and for the networks *A, B, C* and *B*<sub>1</sub> the values of  $M_\infty$  (ratioed to the epoxy–amine phase), the values of  $D$  and the molar enthalpies  $\Delta H$ .

A systematic decrease of water uptakes and a systematic increase of diffusion coefficients are observed in the presence of unreactive or (and) reactive dangling chains (factor  $\geq 2$  between *C* and *A*). At  $P/P_o = 0.3$ , for example, the molar enthalpies increase from 46 to 67 kJ/mol when going from *C* to *A* networks. Furthermore, the values for *B* and *C* are lower than those measured for the untotally cured *C*\* and *B*\* networks.

**Table VI** Dual Mode Sorption Applied to CO<sub>2</sub> Isotherms

	$k_D \left( \frac{\text{cm}^3 \text{ STP}}{\text{cm}^3_{\text{polymer}} \cdot \text{atm}} \right)$	$C'_H \left( \frac{\text{cm}^3 \text{ STP}}{\text{cm}^3_{\text{polymer}}} \right)$	$b$ ( $\text{atm}^{-1}$ )
<i>A</i>	1.02	0	0
<i>B</i>	3.47	2.37	3.52
<i>C</i>	6.91	2.68	8.69

### Permeation Analysis

The water transferred through the sample as a function of time [ $Q = f(t)$ ] has been studied on the *B* sample, under saturated vapor pressure (Fig. 3) and liquid conditions. The permeability  $Pe$  and diffusion coefficients ( $D_{\text{time-lag}}$  and  $D_{\text{slope}}$ ) are given in Table IV according to the eqs. (4) and (5). All the values obtained under pervaporation conditions are the same as those obtained at saturated pressure. Moreover, the  $D_{\text{time-lag}}$  and  $D_{\text{slope}}$  values are nearly the same. These results are opposite to the theory of porous media. Thus, it is clear that the water transport for this type of network corresponds to a diffusion–dissolution mechanism in dense membranes.

The permeability coefficients are surprisingly low, and the diffusion values are 10 times lower than those determined by the sorption method. Two explanations can be proposed: the desorption from the downstream face of the membrane is not fast enough to be considered as instantaneous (the Fick's conditions would not be respected) or the water diffusion under high relative pressures is based on the transport of clusters<sup>16</sup> and not of individual molecules.

## GAS TRANSPORT RESULTS

### Sorption Analysis

The  $\text{CO}_2$  sorption isotherms are shown in Figure 4 for the networks *A*, *B*, *C*. The values of  $M_\infty$  and  $D$  are reported in Table V for  $\text{CO}_2$  pressures of 400 and 700 Torr. The values of  $M_\infty$  decrease by a factor 5 to 6, and those of  $D$  increase by a factor 2.5 when going from *C* to *A*, both in the same trend than water.

The isotherm of the commercial network *A* is linear, which indicates that the Henry's dissolution is mainly acting, without specific interactions even at low pressures.

On the contrary, the isotherms of *B* and *C* are characteristic of the dual mode sorption according to the following equation:

$$C = k_D \cdot P + \frac{(C'_H \cdot b \cdot P)}{(1 + b \cdot P)} \quad (8)$$

$k_D$  is the Henry's constant,  $C'_H$  is the Langmuir's sites concentration, and  $b$  is the affinity constant between the diffusant and the polymer.

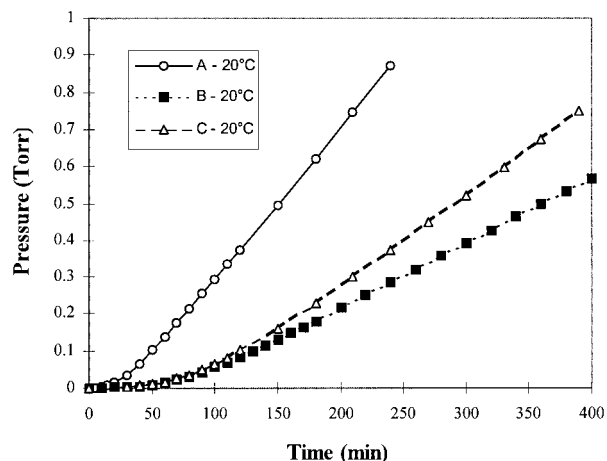


**Figure 5**  $\text{CO}_2$  transport through the networks *A*, *B*, *C*: evolution of the pressure in the downstream compartment as a function of time.

Table VI gives the three parameters obtained by the best fit of the isotherms. The coefficient  $k_D$  highly decreases from 7 to 1 when going from *C* to *A*. The Langmuir's sites concentration decreases until zero for *A* and the affinity coefficient  $b$  is higher for *C* than for *B*. These values are quite imprecise, due to the fact that the microbalance cannot work above the atmospheric pressure. So, the Henry's regime should not be reached.

### Permeation Analysis

Figure 5 shows the amounts of  $\text{CO}_2$ , which have diffused through the networks *A*, *B*, and *C* as a function of time. The coefficients of permeability  $Pe$ , diffusivity  $D$ , solubility  $S$  (calculated from  $Pe/D$ ) are listed in Table VII. The permeabilities are nearly constant, because the diffusion and the sorption coefficients vary with the same factor in the opposite way, the first ones increase, and the second ones decrease when going from *C* to *A*, as previously observed in sorption experiments. Moreover, both values are in the same range as those obtained by sorption experiments, despite very different pressure conditions.

## DISCUSSION

For both water and  $\text{CO}_2$  the evolution of the solubility and diffusion coefficients is significant as a function of the networks composition, and the variations of the two coefficients are opposite.

**Table VII** CO<sub>2</sub> Transport through the Networks *A*, *B*, and *C*: Values of Permeability *Pe*, Diffusion Coefficient *D* and Solubility *S*

	$D \times 10^9$ (cm <sup>2</sup> /s)	<i>Pe</i> (barrer)	$S \times 10^3$ Calculated $\left( \frac{\text{cm}^3 \text{ STP}}{\text{cm}^3_{\text{polymer}} \cdot \text{cmHg}} \right)$
<i>A</i>	1.06	0.24	22.60
<i>B</i>	0.58 (0.34*)	0.14	24.14 (50.68*)
<i>C</i>	0.43 (0.30*)	0.18	41.86 (96.80*)

(\*) Correspondence to the results obtained with sorption experiments.

In the interaction approach, especially in the case of water, the solubility evolution should be related to the concentration of chemical groups able to develop hydrogen bonds: hydroxyl, and also amine groups. If we only consider primary and secondary amine groups, the total concentration of these active groups is the same for all the networks (0.46 mol/100 g). Indeed, an hydroxyl group results from the consumption of an amine function, and the two conditions are verified in all networks:<sup>2</sup> (1) the epoxy-to-amine ratio is stoichiometric; (2) the weight of monoepoxy is precisely half of the diepoxy one.

If we consider now the tertiary amines as potential reactive groups, the total concentration of chemical sites in the fully cured systems *B* and *C* should reach the value of 0.69 mol/100 g corresponding to an increase of 33%. Consequently, in the interaction approach, the solubility cannot be increased more than 33% by the cure cycles, and it should be the same for the fully cured networks *B* and *C*. It is then impossible to explain the very important solubility differences observed between our networks (factor 3 between *A* and *C*, and factor 2 between *B* and *C*).

Thus, an additional contribution can be proposed considering the free volume theory and taking into account the unrelaxed holes present in glassy polymers. In fact, it is known that the free volumes increase with the crosslink density.<sup>17–20</sup> In other words, the unrelaxed holes are less numerous in the presence of dangling chains whatever their origin is (monofunctional epoxy or uncomplete conversion). They represent specific interaction sites for gas at low pressure according to the dual sorption mode, and they act in a similar way than chemical groups. They can explain the evolution of solubility in our networks structural series. Moreover, the opposite evolution of diffu-

sivity is also explained as it is well known that a highly interactive permeate is less mobile.

An interesting confirmation of two types of specific sites is brought by the water calorimetric results because the mean molar interaction energy is not the same for the different networks. We can even show that the unrelaxed holes are less energetic sites: the mean interaction energy decreases from 67 to 46 kJ/mol when the unrelaxed holes concentration increases.

## CONCLUSION

We have analyzed the water and gas transport properties of a series of epoxy–amine stoichiometric networks that differ by the cure cycle but almost by the presence of monoepoxy in place of diepoxy. The monoepoxy has been chosen to have a similar chemical structure as DGEBA, and the same massic oxirane concentration, thus leading to the same chemical site concentration, especially in the fully cured systems.

We have shown through seven networks that the solubility coefficients decrease, and the diffusivity coefficients and the molar energies (for water) increase when the cure cycle is uncomplete or when the monoepoxy/diepoxy ratio increases. The magnitude of all these evolutions cannot be explained by the lonely chemical interaction approach.

Thus, two types of specific sites have been taken into account:<sup>21–23</sup> the polar groups, and the unrelaxed holes. The last ones depend on the free volumes, which increase with crosslink density. Their interaction energy towards the diffusing mol is lower than that of the chemical polar groups.



In our model series, we can conclude that the evolution of unrelaxed holes governs the evolution of the transport properties.

## REFERENCES

1. Sabra, A. S. *Polymer* 1987, 28, 1030.
2. Bellenger, V.; Verdu, J.; Morel, E. *J Mater Sci* 1989, 24, 63.
3. Ellis, T. S.; Karasz, F. E. *Polymer* 1984, 25, 664.
4. Klotz, J. *Polym Eng Sci* 1996, 36, 1129.
5. Apicella, A.; Nicolais, L. *Adv Polym Sci* 1985, 72, 69.
6. Johncock, P.; Tudgey. *Br Polym J* 1986, 18, 292.
7. Park, G. S. In *Diffusion in Polymers*; Crank, J.; Park, G. S., Eds.; Academic Press: London, 1968; p. 1.
8. Crank, J.; Park, G. S.; Stanett, V. In *Diffusion in Polymers*; Crank, J.; Park, G. S., Eds.; Academic Press: London, 1968; p. 1.
9. Paul, D. R. *J Polym Sci A-2 Polym Phys Ed* 1969, 7, 1811.
10. Petropoulos, J. H. *J Polym Sci A-2 Polym Phys Ed* 1970, 8, 1797.
11. Paul, D. R.; Kouros, W. J. *J Polym Sci A-2 Polym Phys* 1976, 14, 675.
12. Fujita, H. In *Diffusion in Polymers*; Crank, J.; Park, G. S., Eds.; Academic Press: London, 1968; p. 75.
13. Barrer, R. M. *Trans Faraday Society* 1939, 35, 628.
14. Daynes, H. *Proc R Soc* 1920, A97, 286.
15. Beaudoin, Confidential document of CEA 1996.
16. Bungay, P. M.; Lonsdale, H. K.; De Pinho, M. N. *ASI Series, Series C: Math Phys Sci* 1986, 181.
17. Yang, Y. *J Polym Sci Part A Polym Chem* 1986, 24, 2609.
18. Enns, J. B.; Gillham, J. K. *J Appl Polym Sci* 1983, 28, 2831.
19. Morgan, R. J.; O'Neal, J. E.; Miller, D. B. *J Mater Sci* 1979, 14, 109.
20. Wong, E. S.; Broutman, L. *J Polym Eng Sci* 1985, 25, 529.
21. Aronhime, M. T.; Peng, X.; Gillham, J. K.; Small, R. D. *J Appl Polym Sci* 1986, 32, 3589.
22. Min, B. G.; Shin, D. K.; Stachurski, Z. H.; Hodgkin, J. H. *Polym Bull* 1994, 33, 465.
23. Diamant, Y.; Marom, G.; Broutman, L. J. *J Appl Polym Sci* 1981, 26, 3015.